Rainbow-trapping absorbers for transmission problems: Broadband and perfect sound absorbing panels

Jean-Philippe Groby, Vincent Pagneux , Vicente Roméro-Garcia
Laboratoire d'Acoustique de l'Université du Maine (LAUM), UMR CNRS 6613, Av. Olivier Messiaen, 72085 Le Mans cedex 9, France.

Noé Jimenez
Instituto de Instrumentación para Imagen Molecular (I3M), Centro Mixto CSIC - Universitat Politècnica de València, Camino de Vera s/n, 46022 Valencia, Spain.

Summary
Broadband and perfect sound absorption by subwavelength panels for transmission problems is reported. The asymmetric panels are composed of a periodic array of open waveguides loaded by Helmholtz resonators (HRs) with slightly different dimensions along the structure depth. In each waveguide, the deepest resonator generates a low cut-off frequency, reducing drastically the transmission. The geometry of the preceding HR is designed to possess a slightly higher resonance frequency and is tuned to match the structure impedance with the surrounding one, thanks to the critical coupling condition. Therefore, reflection vanishes and the structure becomes critically coupled to the incident wave, resulting in perfect sound absorption. This process is repeated by adding HRs, whose resonance frequency is slightly higher than the preceding one, to each waveguide. The last added HR fixes the high cut-off frequency of the perfect absorption band in such a way that slow sound condition is achieved within each open waveguide over a broadband frequency range. We experimentally, theoretically and numerically report perfect sound absorption for two panels: (1) at 300 Hz for a transparent panel of total thickness 2.8 cm, i.e., 40 times smaller than the wavelength, (2) from 350 to 1000 Hz for a transparent panel composed of 9 resonators with a total thickness of 12 cm, i.e., 10 times smaller than the wavelength and covering almost two octaves.

1. Introduction

Perfect acoustic absorption has been reported in rigidly-backed subwavelength structures by using slow sound and QWRs [1] or HRs [2], or by using membranes and plates [3, 4, 5, 6]. However, until now, only a few works present broadband perfect absorption in rigid-backed metamaterials. One kind of these broadband absorbers are metaporous materials [7, 8, 9, 10], whose low frequency performance is limited by the inertial regime of the porous matrix material.

When the system is not rigidly backed and transmission is allowed, the scattering matrix presents two different eigenvalues. In order to obtain perfect absorption for one-sided incident wave both eigenvalues must vanish at the same frequency [12]. This implies that symmetric and antisymmetric modes must be simultaneously critically coupled at a given frequency [11]. In the case in which the eigenvalues are both zero but at different frequencies, then the system cannot present perfect absorption, but quasi-perfect absorption can be achieved by approaching the symmetric and antisymmetric modes using strong dispersion [13]. Perfect acoustic absorption can be obtained by using degenerate resonators, where monopolar and dipolar resonances can be excited at the same frequency [14]. Another strategy consists in using asymmetric graded materials, e.g., chirped layered porous structures [15], but these structures lack of subwavelength resonances and therefore its thickness is of the order of half of the incoming wavelength. A final configuration to achieve perfect absorption in transmission consists in breaking the symmetry of the structure by making use of double-interacting resonators [12].

In this work, we address the problem of perfect and broadband acoustic absorption including transmission using deep subwavelength structures, which to our knowledge was never addressed before. To do so, we designed panels composed of monopolar resonators

(c) European Acoustics Association

Copyright © 2018 | EAA – HELINA | ISSN: 2226-5147
All rights reserved

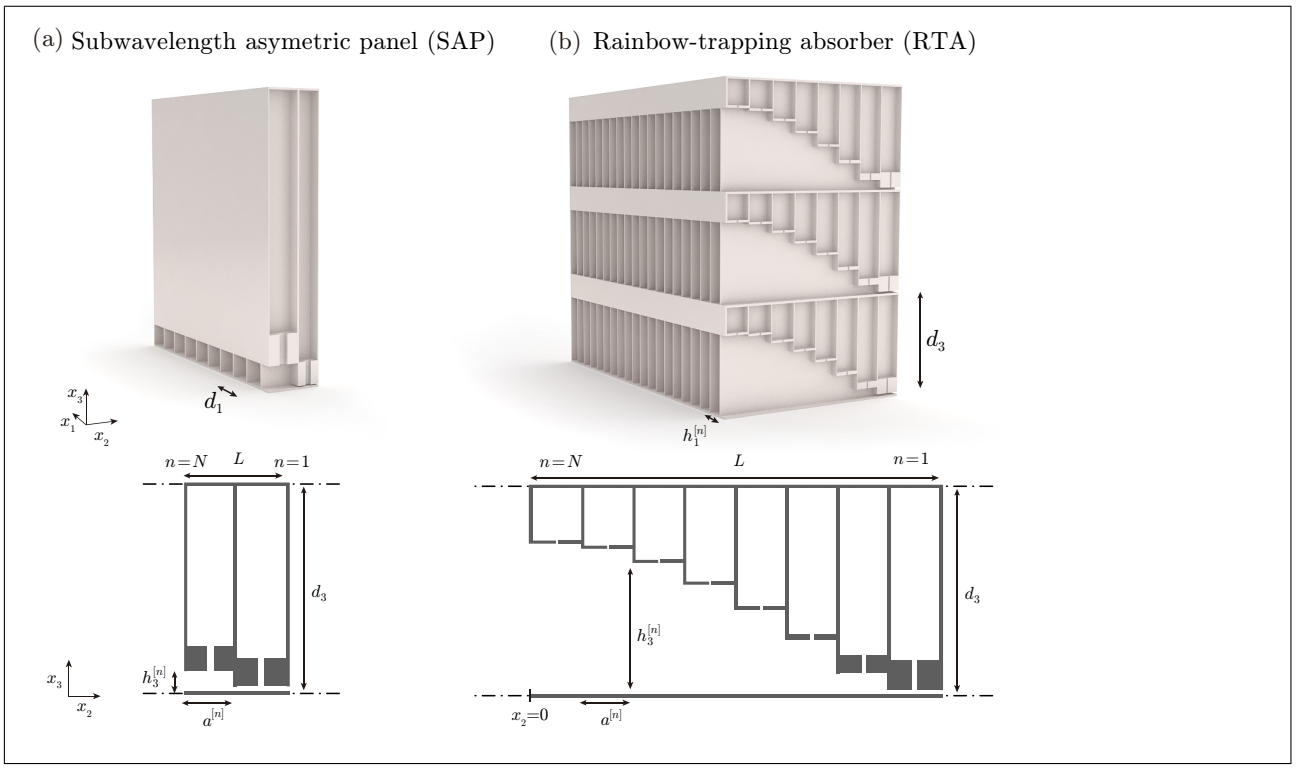


Figure 1. (a) Conceptual view of a subwavelength asymmetric panel (SAP) ($N = 2$ resonators), where cross-section shows the waveguide and the loading HRs. (b) Conceptual view of a rainbow trapping absorber (RTA) with $N = 8$ HRs. Scheme showing the geometrical variables for (c) the SAP and (d) RTA panels.

with graded dimensions, namely *rainbow-trapping absorbers*. These panels present broadband, perfect and asymmetric sound absorption, and, due to slow sound, their thickness is reduced to the deep-subwavelength regime. Rainbow trapping phenomenon, i.e., the localization of energy due to a gradual reduction of the group velocity in graded structures, has been observed in optics [16], acoustics [17, 18] or elastodynamics [19]. However, losses were not accounted for and, therefore, absorption was not studied in these works.

2. System description

The structures are composed of a rigid panel, of thickness L, periodically perforated with series of identical waveguides of variable square cross-section loaded by an array of N HRs of different dimensions, as shown in Figs. 1 (a, b). Each waveguide is therefore divided in N segments of length $a^{[n]}$, width $h_1^{[n]}$ and height $h_3^{[n]}$. The HRs are located in the middle of each waveguide section.

Two samples were designed. The first one, namely *subwavelength asymmetric panel* (SAP) was composed of $N = 2$ HRs and it is shown in Fig. 1 (a). The second one, namely *rainbow-trapping absorber* (RTA) was composed first, in a design stage, by $N = 8$ and, finally, $N = 9$ HRs for the experimental tests, as shown in Fig. 1 (b). The SAP was designed to produce a single-frequency peak of perfect absorption while the RTAs were designed to exhibit broadband perfect absorption.

The geometrical parameters of both structures were tuned using optimization methods (sequential quadratic programming (SQP) [**?**]). In the case of the SAP ($N = 2$) the cost function minimized during the optimization process was $\varepsilon_{\mathrm{SAP}} = |R^-|^2 + |T|^2$, i.e., to maximize the absorption at a given frequency, in this case we selected 300 Hz. The length of the SAP was constrained to $L = 2.64$ cm, i.e., a panel 40 times thinner than the incoming wavelength. In the case of the rainbow trapping absorber ($N = 9$), the cost function was $\varepsilon_{\mathrm{RTA}} = \int_{f_1}^{f_N} |R^-|^2 + |T|^2 df$, i.e., to maximize the absorption in a broad frequency bandwidth, that was chosen from $f_1 = 300$ to $f_N = 1000$ Hz. In the case of the RTA the length of the panel was constrained to $L = 11.3$ cm, i.e. a panel 10 times thinner than the wavelength at 300 Hz. The geometrical parameters obtained by the optimization process are given in the A.

3. Subwavelength asymmetric panel (SAP)

We start analysing the behaviour of the designed SAP with $N = 2$ HRs, considering the two directions of incidence, namely *forward* and *backward*, as depicted in Figs. 2 (a,b). Figures 2 (c-f) show the corresponding

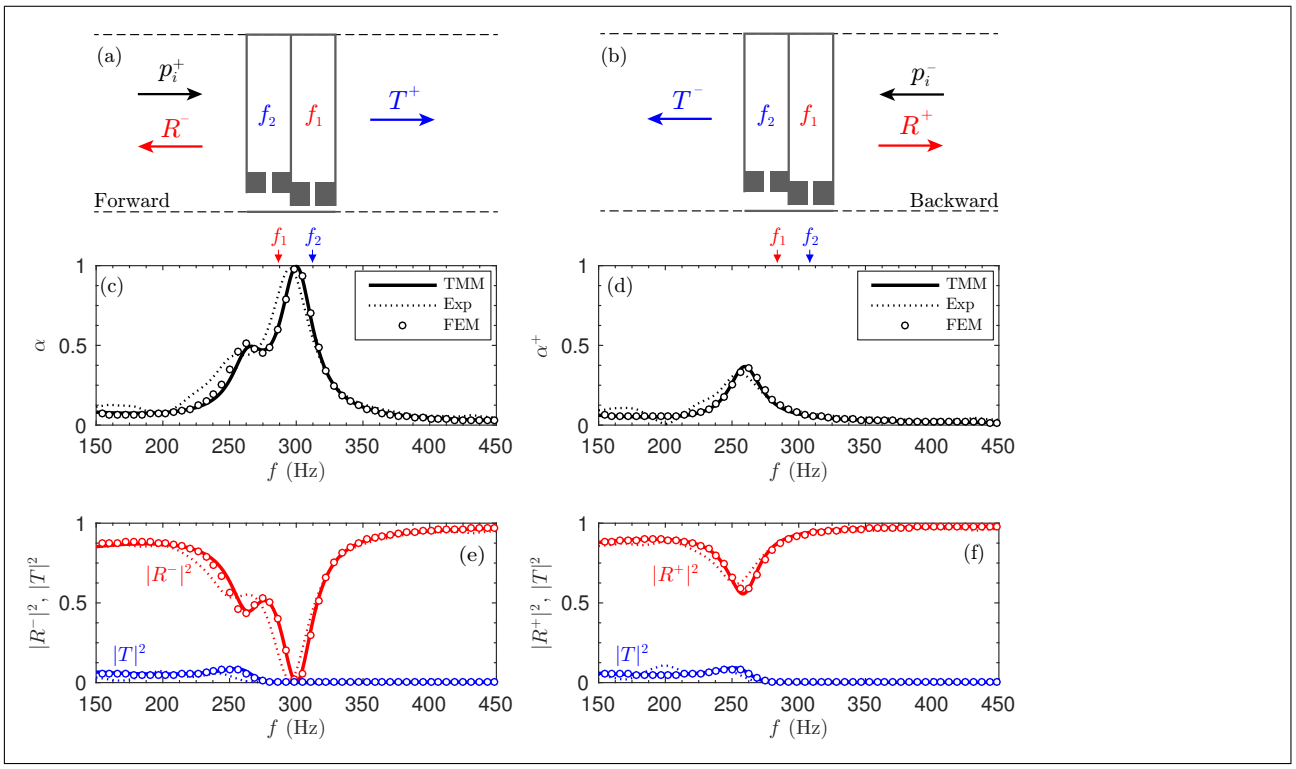


Figure 2. Scheme of the subwavelength asymmetric panel in (a) forward and (b) reverse configuration. (c) Absorption for the forward configuration obtained using TMM (continuous line), FEM (circles), and experiment (dotted line). Corresponding reflection and transmission coefficients. (d) Absorption for the backward configuration. (f) Corresponding reflection and transmission coefficients. The arrows mark the resonance frequencies of the HRs, f_1 and f_2.

absorption, reflection and transmission coefficients for each case.

First, in the forward configuration, shown in Fig. 2 (a), the resonator $n = 1$ of the waveguide presents a resonance frequency at $f_1 = 285$ Hz. As a consequence, above f_1, a band gap is introduced and the transmission is strongly reduced, the HR acting effectively as a rigidly-backed wall for the right ingoing waves. Then, the resonator $n = 2$, with a superior resonance frequency at $f_2 = 310$ Hz, is tuned by the optimization process to critically couple the system with the exterior medium, matching the impedance of the waveguide to that of the surrounding medium. This is achieved at 300 Hz. As a consequence, no reflected waves are produced at this particular frequency and therefore, $\alpha = 1-|R^-|^2-|T|^2 = 1$ holds. In this situation, perfect absorption is observed in a panel 40 times thinner than the wavelength, i.e., a panel of thickness $L = 2.64$ cm. It is worth noting here that the change of section in the main waveguide helps to achieve the impedance matching, specially for very thin SAPs as the one presented here.

Second, in the backward propagation shown in Fig. 2 (b), the wave impinges first the lowest resonance frequency resonator, f_1. Now at 300 Hz the wave almost no transmission is allowed in the waveguide. As the waveguide is not impedance matched at 300 Hz in backward direction, reflection is high and absorption is poor ($\alpha^+ = 0.05$). For frequencies below f_2, propagation is allowed in the main waveguide and the effect of the second HR may be visible inducing a decrease of the reflection coefficient. However, the impedance matching in the backward direction is not fully achieved and only a small amount of absorption is observed near the resonance frequency of the first resonator. Therefore, the absorption in this configuration is highly asymmetric.

4. Rainbow-trapping absorbers (RTA)

The concept of the SAP can be applied to design broadband perfect absorbers. The idea is to create a frequency-cascade of band-gaps and critically coupled resonators and, thus, generate a rainbow-trapping effect. The process is as follows. First, we tune the deepest resonator ($n = 1$) in the waveguide to reduce the transmission above a frequency f_1. Second, in the same way as previously done in the SAP, a second resonator with slightly higher resonance frequency, f_2, is placed in the preceding segment of the waveguide. The geometry of this resonator and the section of the waveguide are tuned to impedance match the system at this frequency. Therefore, the reflection vanishes and a peak of perfect absorption is achieved in the same way as in the SAPs. Note this latter HR also reduces the transmission at even higher frequencies.

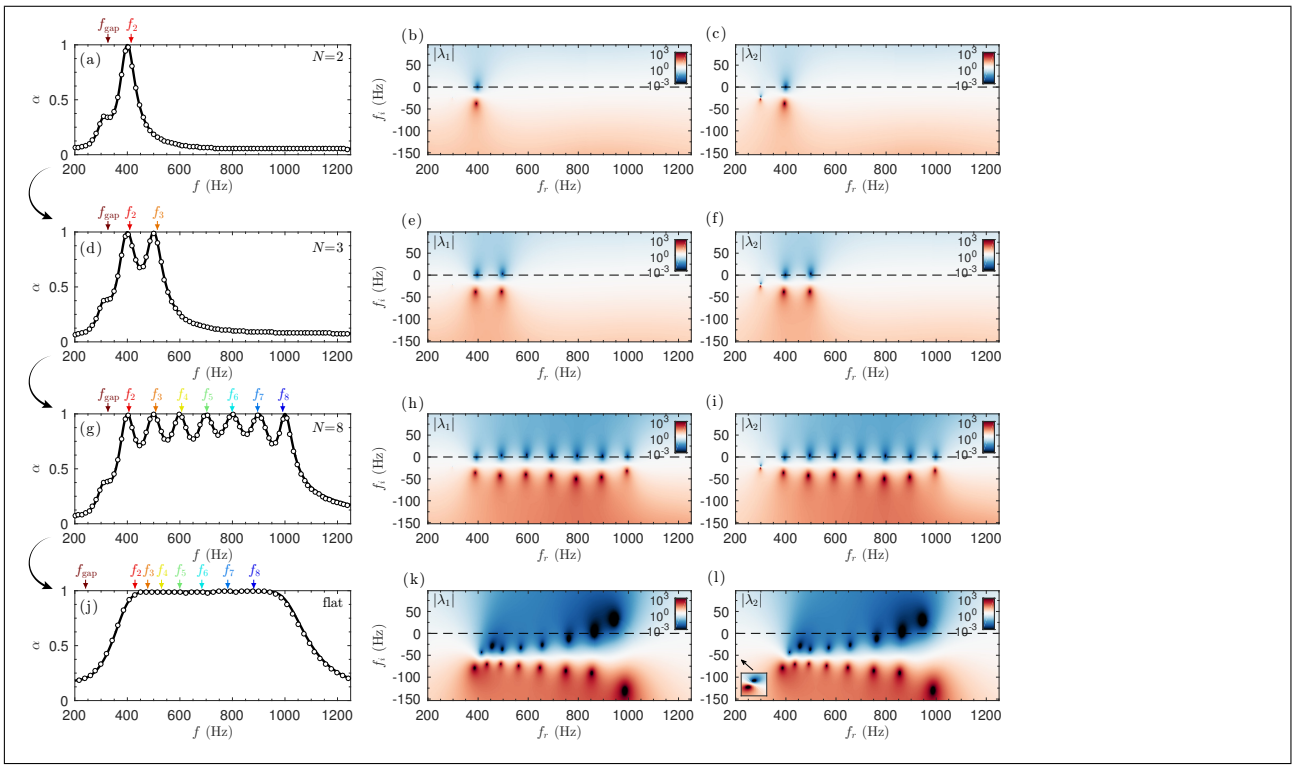


Figure 3. Process to critically couple the rainbow-trapping absorbers. (a) Absorption using $N = 2$ HRs obtained using TMM (continuous lines) and FEM simulations (markers), (b-c) corresponding complex frequency plane representation of the eigenvalues of the scattering matrix. (d) Absorption using $N = 3$ HRs and (e-f) corresponding complex frequency plane. (g) Absorption using $N = 8$ HRs and (h-i) complex frequency plane. (j) Optimized broadband and flat absorption using $N = 8$ HRs, (k-l) corresponding complex frequency plane.

Then, the process can be repeated by extending the waveguide with more segments, each one with a tuned HR being its resonance frequency higher than the preceding one.

5. Conclusions

We reported perfect acoustic absorption over a broad frequency band in deep-subwavelength thickness panels including transmission using the rainbow-trapping effect. In particular, we first presented monochromatic perfect absorption for a subwavelength asymmetric panel (SAP) 40 times smaller than the incoming wavelength (2.64 cm at 300 Hz) using two double-interacting Helmholtz resonators. Then, we reported flat and perfect absorption over a frequency range covering from 300 to 1000 Hz, i.e., almost two octaves, using a rainbow-trapping absorber (RTA) composed of nine resonators and ten times smaller than the wavelength at 300 Hz (11.3 cm). We showed that to obtain broadband and perfect absorption in the transmission problem, three conditions must be simultaneously fulfilled: (*i*) the zeros of the eigenvalues of the scattering matrix must be located on the real frequency axis, (*ii*) the zeros of both eigenvalues, $\lambda_{1,2}$, must be at same frequencies, and, (*iii*) the quality factor of the resonances must be low to overlap in frequency. These three conditions are mandatory to maximize the broadband absorption of the panels and were satisfied by the optimization process.

For more information, the readers can read the full paper [20].

Acknowledgement

The authors acknowledge financial support from the Metaudible Project ANR-13-BS09-0003, cofunded by ANR and FRAE. This article is based upon work from COST Action DENORMS CA15125, supported by COST (European Cooperation in Science and Technology)

A. Geometrical parameters

The geometrical parameters for the SAP ($N = 2$), corresponding to Fig. 2, are listed in Table I. The total structure thickness is $L = \sum a^{[n]} = 28.6$ mm, and its height and width of the unit cell are $d_3 = 148.1$ mm and $d_1 = 14.8$ mm respectively.

The geometrical parameters for the RTA ($N = 8$), corresponding to Fig. 3 (j-l), are listed in Table II. The total structure thickness is $L = 120$ mm, and its height and width of the unit cell are $d_3 = 48.7$ mm and $d_1 = 6.3$ mm respectively.

Table I. Geometrical parameters for the SAP ($N = 2$).

n	$a^{[n]}$ (mm)	$h_3^{[n]}$ (mm)	$h_1^{[n]}$ (mm)	$l_{\mathbf{n}}^{[n]}$ (mm)	$l_{\mathbf{c}}^{[n]}$ (mm)	$w_{\mathbf{n}}^{[n]}$ (mm)	$w_{\mathbf{c},1}^{[n]}$ (mm)	$w_{\mathbf{c},2}^{[n]}$ (mm)
2	16.8	12.7	13.8	15.4	119.1	4.5	13.8	15.7
1	11.8	1.0	13.8	12.0	134.1	3.2	13.8	10.8

Table II. Geometrical parameters for the RTA ($N = 8$).

n	$a^{[n]}$ (mm)	$h_3^{[n]}$ (mm)	$h_1^{[n]}$ (mm)	$l_{\mathbf{n}}^{[n]}$ (mm)	$l_{\mathbf{c}}^{[n]}$ (mm)	$w_{\mathbf{n}}^{[n]}$ (mm)	$w_{\mathbf{c},1}^{[n]}$ (mm)	$w_{\mathbf{c},2}^{[n]}$ (mm)
8	15.0	28.8	5.3	1.0	17.9	0.8	5.3	13.5
7	15.0	27.4	5.3	1.2	19.2	0.8	5.3	14.0
6	15.0	25.9	5.3	1.5	20.3	0.8	5.3	14.0
5	15.0	24.5	5.3	1.8	21.3	0.8	5.3	14.0
4	15.0	23.1	5.3	2.2	22.4	0.7	5.3	14.0
3	15.0	22.1	5.3	2.6	23.0	0.7	5.3	14.0
2	15.0	21.9	5.3	3.2	22.6	0.7	5.3	14.0
1	15.0	0.8	0.8	5.7	41.2	0.7	5.3	13.5

References

[1] Groby J P, Pommier R and Aurégan Y 2016 *J. Acoust. Soc. Am.* **139** 1660–1671

[2] Jiménez N, Huang W, Romero-García V, Pagneux V and Groby J P 2016 *Applied Physics Letters* **109** 121902

[3] Yang Z, Mei J, Yang M, Chan N and Sheng P 2008 *Phys. Rev. Lett.* **101** 204301

[4] Mei J, Ma G, Yang M, Yang Z, Wen W and Sheng P 2012 *Nat. Commun.* **3** 756

[5] Ma G, Yang M, Xiao S, Yang Z and Sheng P 2014 *Nat. Mater.* **13** 873–878

[6] Romero-García V, Theocharis G, Richoux O, Merkel A, Tournat V and Pagneux V 2016 *Sci. Rep.* **6** 19519

[7] Groby J P, Duclos A, Dazel O, Boeckx L and Lauriks W 2011 *J. Acoust. Soc. Am.* **129** 3035–3046

[8] Lagarrigue C, Groby J, Tournat V, Dazel O and Umnova O 2013 *J. Acoust. Soc. Am.* **134** 4670–4680

[9] Boutin C 2013 *J. Acoust. Soc. Am.* **134** 4717–4729

[10] Groby J P, Lagarrigue C, Brouard B, Dazel O, Tournat V and Nennig B 2015 *J. Acoust. Soc. Am.* **137** 273–280

[11] Piper J R, Liu V and Fan S 2014 *Appl. Phys. Lett.* **104** 251110

[12] Merkel A, Theocharis G, Richoux O, Romero-García V and Pagneux V 2015 *Appl. Phys. Lett.* **107** 244102

[13] Jiménez N, Romero-García V, Pagneux V and Groby J P 2017 *Phys. Rev. B* **95** 014205

[14] Yang M, Meng C, Fu C, Li Y, Yang Z and Sheng P 2015 *Appl. Phys. Lett.* **107** 104104

[15] Jiménez N, Romero-García V, Cebrecos A, Picó R, Sánchez-Morcillo V J and García-Raffi L M 2016 *AIP Advances* **6** 121605

[16] Tsakmakidis K L, Boardman A D and Hess O 2007 *Nature* **450** 397–401

[17] Zhu J, Chen Y, Zhu X, Garcia-Vidal F J, Yin X, Zhang W and Zhang X 2013 *Scientific reports* **3** 1728

[18] Romero-Garcia V, Picó R, Cebrecos A, Sanchez-Morcillo V and Staliunas K 2013 *Applied Physics Letters* **102** 091906

[19] Colombi A, Colquitt D, Roux P, Guenneau S and Craster R V 2016 *Scientific reports* **6** 27717

[20] Jimenez, N. Romero-Garcia, V. Pagneux, V. and Groby J.-P. 2016 *Scientific reports* **2** 13595